A Study of the Catalysed Pyrolysis of Date Stone Biomass in Fixed Bed Conditions

Hatem M

Chemical engineering, Cardiff University

Abstract: Date palm is one of the main agricultural products in the Saudi Arabia, it has been playing a significant role in the daily life of the people in the Middle East and North Africa for the last seven thousand years. Saudi Arabia is the third largest global producer of dates, while Egypt occupies the number of one position as the largest date producer across the world. the total production of date in 2018 in Saudi Arabia was reported at 1,399,762 metric tonnes in 2018 from an estimated 30,429,607 trees, which were cultivated in an estimated area of 155,118 hectares.

The impact of catalyst particle and its associated size on the pyrolysis of date stone is discussed in this section. The study is conducted on different types of catalysts and at various conditions (biomass to catalyst ratios) at fixed bed conditions. The main aim of the study s to understand the consequences of changing the type of catalyst, the ratio of catalysts, and particle sizes on the kinetic behavior from the system while investigating the effects on the biomass pyrolysis.

KEYWORDS: Date stone, TGA, pyrolysis.

DOI of the Article: https://doi.org/10.46501/IJMTST0708032

Available online at: http://www.ijmtst.com/vol7issue08.html

As per UGC guidelines an electronic bar code is provided to seure your paper

To Cite this Article: Hatem M. A Study of the Catalysed Pyrolysis of Date Stone Biomass in Fixed Bed Conditions. *International Journal for Modern Trends in Science and Technology* 2021, *7*, 0708056, pp. 193-200. https://doi.org/10.46501/IJMTST0708032

Article Info. Received: 09 July 2021; Accepted: 07 August 2021; Published: 17 August 2021

INTRODUCTION

The Thermal decomposition of a range of date stone biomass particle sizes conditions was investigated under inert conditions. The investigation was done using a thermogravimetric analyser (TGA) device.

The material's mass is monitored with respect to time and temperature to conclude a thermogravimetric analysis (TGA). The technique works best when a sample material is exposed to a controlled environment. TGA is often used to study the thermal behaviour in various process, such as gasification, combustion and pyrolysis. It determines the mass loss characteristics of the biomass in a range of heating rates between 0 to 60 ℃ per minute and provides accurate results in temperatures up to 1300 ℃ in in an atmosphere environment. TGA can be used in investigating the degradation mechanism and reaction kinetics of biomass in a thermochemical conversion process. The analysis provides data that can be used to plot a thermogravimetric (TG) curve, which illustrates the dynamic mass decay against temperature and/or time. Differentiating the data results in differential thermogravimetric data (DTG) which can be used to indicate the biomass conversion rate during the thermal process.

Fixed bed Thermogravimetric analysis (TGA)

The results of pyrolysis via thermogravimetric analysis can be represented as a function of x, as shown on Eq. (1).

$$\times = \frac{mo-m}{mo-mf} \text{Equation - 1}$$

Where:

mo: the initial mass of the sample.

m: the instantaneous mass of the pyrolysis sample.

mf: the final residual mass.

The degree of conversion with respect to the temperature at a constant rate of heating at 20 ℃/min at 4 date stone particles sizes obtained is shown in Figure (5-1). The figure shows that at temperatures lower than 250 ℃, a change in mass is observed as a result of moisture loss at the early heating period. At 250 ℃, the date stone thermal decomposition commenced, however the active pyrolysis (i.e. the primary decomposition stage) occurred at temperatures between 260 ℃ to 400 ℃. Most of the volatile decomposition occurred at the same temperature range, consisting of up to 80% of the total mass conversion. Consequently, when the conversion rate exceeds 80%, char is mostly what remains thereafter. As per the TGA results, the same trend was observed at all particles sizes, and therefore it is proposed that under the conditions studied, the particle size is independent of the decomposition rate.

Four particle sizes were used in the experiments to investigate their effect on the pyrolysis process, as shown on Figure (1). It showed that TGA is not heavily influenced by the changes in the date stone sizes, as long as the same biomass material was used. This is not surprising, as it was also observed in other biomass materials, such as the marine biomass (codiumfagile) as shown by Daneshvar et al. who tested particle sizes ranging from 75 μm - 1400 μm [1].

The biomass used consists of hemicellulose, cellulose and lignin, which each has distinctively different structures. Therefore, they can be identified via the thermogravimetric analysis [2].Hemi-cellulose decomposes at a temperature range of 220 ℃ and 315 ℃, while cellulose decomposes at 315 ℃ and 400 ℃ and lignin decomposes at a much wider temperature range between 160 to 900 ℃; according to Yang et al. [3].

The differential rate of conversion (dm/dt) was measured at a heating rate of 20 ℃/min via the differential thermogravimetric analysis method (DTG). The analysis was observed for particle sizes of 300, 500, 600 and 710 μm, shown on Figure (2) with respect to the distribution curves (DTG) of the date stones. The first peak is seen at 100 ℃ which corresponds to the sample's moisture content. The second peak is seen between 200 ℃ to 300 ℃, indicating the hemicellulose decomposition. The last peak is seen at temperatures between 300 ℃ to 380 ℃ and is likely a represented of the cellulose decomposition. The mass loss was lower and at a more consistent rate when temperature exceeded 380 ℃, relatively to the decomposition of lignin.

This is similar to the DTG analysis done by E.Kastanki et al for the pyrolysis of date stone [4] and Jae et al. for maple wood [5].

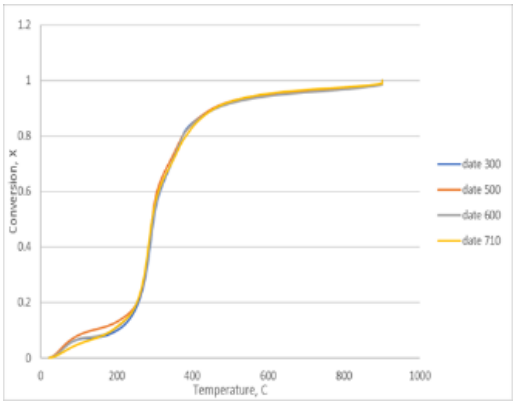

Figure 1 Relationship between mass conversion and temperature for date stone of different particle sizes. Heating rate 20°C/min, sample wt. ~10mg (TGA), nitrogen flow rate 100 ml/min.

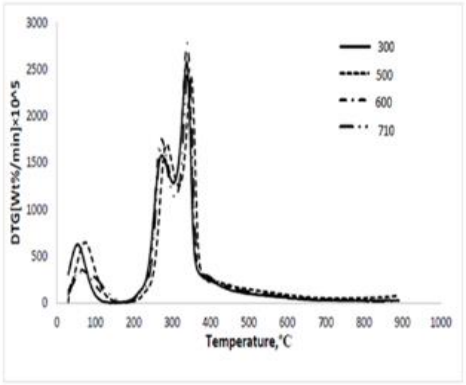

Figure 1 Variation of the instantaneous rate of reaction with temperature at 20℃/min heating rate for pyrolysis of date stone.

Kinetic analysis of pyrolysis of Date stone

The date stone was tested at non-isothermal conditions in the TGA at a heating rate of 20 ℃/min at various solid-state mechanisms, outlined on Table (1). The tests were conducted to determine the mechanism using the Coats Redfern method. The result of the test is to determine the mechanisms leading to the particle size (710 μm) decomposition, at a conversation rate (x) ranging between 0.2 to 0.8 because the main conversion occurs in this study range.

Table 1 Typical Reaction Mechanism for Heterogeneous Solid-State Reaction [6].

Symbol	*Reaction mechanism*	*f(x)*	G(x)
G1	One-dimensional diffusion, 1D	1/2x	x2
G2	*Two- dimensional diffusion, (Valensi)*	[-ln(1-x)]-1	x+(1-x)ln(1-x)
G3	*Three-dimensional diffusion, (Jander)*	1.5(1-x)2/3[1-(1-x)1/3]-1	[1-(1-x)1/3]2
G4	*Three-dimensional diffusion, (G-B)*	1.5[1-(1-x)1/3]-1	1-2x/3-(1-x)2/3
G5	*Three-dimensional diffusion(A-J)*	1.5(1+x)2/3[(1+x)1/3-1]-1	[(1+x)1/3-1]2
G6	*Nucleation and growth(n=2/3)*	1.5(1-x)[-ln(1-x)]1/3	[-ln(1-x)]2/3
G7	*Nucleation and growth (n=1/2)*	2(1-x)[-ln(1-x)]1/2	[-ln(1-x)]1/2
G8	*Nucleation and growth (n=1/3)*	3(1-x)[-ln(1-x)]2/3	[-ln(1-x)]1/3
G9	*Nucleation and growth(n=1/4)*	4(1-x)[-ln(1-x)]1/3	[-ln(1-x)]1/4
G10	Autocatalytic reaction	x(1-x)	ln[x/(1-x)]
G11	*Mampel power law(n=1/2)*	2x1/2	x1/2
G12	*Mampel power law(n=1/3)*	3x2/3	x1/3
G13	*Mampel power law(n=1/4)*	4x3/4	x1/4
G14	*Chemical reaction(n=3)*	(1-x)3	*[(1-x)-2-1]/2*
G15	*Chemical reaction(n=2)*	(1-x)2	*(1-x)-1-1*
G16	*Chemical reaction(n=1)*	1-x	*-ln(1-x)*
G17	*Chemical reaction(n=0)*	1	x
G18	*Contraction sphere*	3(1-x)2/3	1-(1-x)1/3
G19	Contraction cylinder	2(1-x)1/2	1-(1-x)1/2
Note: A-J: Anti- Jander; G-B: Ginstling-Brounshtein			

The analysis was conducted using Equation (2), which was applied to each individual model. The function G(x) which yields a straight line alongside the highest correlation coefficient is the best representation of the mass loss reaction's kinetic.

$$ln\left(\frac{G(x)}{T2}\right) = ln\left(\frac{AR}{\beta E}\right) - \frac{E}{RT} \quad \text{Equation 2}$$

The values of G(x) and the correspondent correlation coefficient are shown on Table (5-2). This is obtained via plotting the ln(G(x)/T2) with respect to (1/T), shown on Figure (3). The value of the activation energy can be obtained as the value of each line.

Table 2 Reaction model for date stone decomposition during fixed bed non-isothermal pyrolysis.

NON-ISOTHERMAL (TGA), X=0.2-0.8									
G(X)	**G1**	**G2**	**G6**	**G7**	**G14**	**G15**	**G16**	**G17**	**G18**
R2	0.82	0.85	0.91	0.88	0.97	0.94	0.88	0.75	0.87
EA	48.3	55.99	83.1	43.7	73.84	51.28	32.94	19.26	4.27

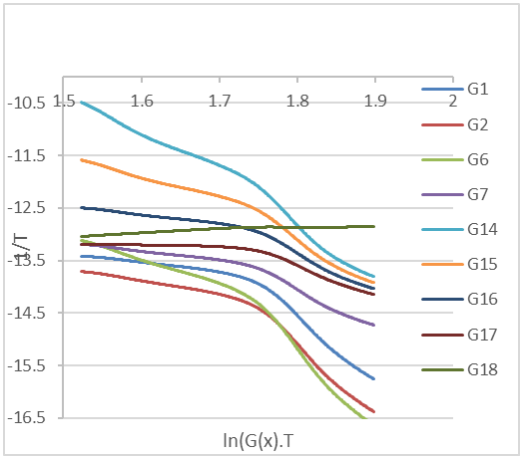

Figure 1 Correlation of ln(G(x)/T) versus 1/T for 710 μm particle size for non-isothermal TGA.

The universal kinetics of the thermal decomposition of biomass can be described using Equation (5-3), which is possible as the pyrosis process is a heterogenous solid-state reaction [7].

$$\frac{dX}{dt}=k(Cg,T)f(X) \quad \text{Equation 3}$$

Where:

T: temperature of the reaction

t: time of the reaction

Cg: the concentration of the gasification agent.

f(x): the differential reaction model.

k(T): the time dependent reaction rate, obtain by Equation (4).

$$K = A \exp\left[\frac{-Ea}{RT}\right] \quad \text{Equation 4}$$

The reaction rate of the gasification can be considered solely dependent on temperature, if thegasification agent (Cg) concentration remained a constant during the reaction. This was assumed for the following calculations.

Various experimental techniques were utilised at the TGA non-isothermal process. The goal is to examine changes in the sample as the temperature increases. The rate constant (k) is directly proportional to temperature. This eliminates the need of multiple experiments as it allows activation energy derivation from a single experiment [8].

Non-isothermal thermogravimetric analysis was compared to the appropriately fitting and free models. The reaction mechanism was determined by the first approach at Table (1). Substituting the Arrhenius equation within equation (5) yields the following.

$$\int\frac{dx}{f(x)}=\int k(T)dt \quad \text{Equation 5}$$

$$\int\frac{dx}{f(x)}=\int A \exp\frac{-E}{RT}\,dt \quad \text{Equation 6}$$

Where:

β heating is rate,

To is the initial temperature of the reaction.

Differentiating both sides of equations (6) and (7) above yields Equation (8). Which upon combining with Equation (6) results in Equation (9).

$$dT=\beta dt \text{ or } dt=dT/\beta \quad \text{Equation 7}$$

$$\int\frac{dx}{f(x)}=\int_0^T A\beta exp-\frac{E}{RT}dT \quad \text{Equation 8}$$

The right-hand side is a non-integrable function, however the left side of equation is again G(x).

$$G(X) = \int_0^T A\beta exp-\frac{E}{RT}dT \quad \text{Equation 9}$$

Equation (5- 11) describes the Frank-Kaminski approximation equation which can be used to select the reaction mechanism model.

$$\int_0^T exp\left(-\frac{E}{RT}\right)dt = \frac{RT^2}{E}exp(-\frac{E}{RT}) \quad \text{Equation 10}$$

Merging Equations (9) and (10) results equation (11) which is called the Coats-Redfern equation [9]. The Coats-Redfern integral method is in fact a single heating rate method which is used widely for the analysis of kinetic parameters of non-isothermal systems [10]. The method when applied, it yielded Equation (12) as following:

$$\text{Ln}(\frac{G(x)}{T^2}) = ln\left(\frac{AR}{\beta E}\right)-\frac{E}{RT} \quad \text{Equation 11}$$

Finally, plotting Ln ((G(x))/T^2)againt 1/T yields a straight line with (-E/R) slope. Indicating that ln (AR/βE) is a constant. The mechanism function G(x) takes into account the reaction mechanism. Using a model from Table (1) and substituting in Equation (12), the mechanism function model can be confirmed, and was found to describe the linear nature of the reaction as per the Pearson correlation coefficient R2. The main goal of this study is to quantify the pyrolysis kinetics of palm stone in a batch reaction. The model selected to describe the mechanisms of the reactions with respect to the highest value of regression on the test model. This is to allow estimation of activation energy.

THE SELECTION OF CATALYST MATERIAL

It is important to ensure the correct catalyst material is selected for the experiments, as it will have a big impact on the reactions within the gasifier and the used TGA device [11][12].

Pinto et al. [13] studied the effectiveness of lime, olivine, and dolomite, and found dolomite was the most effective catalyst to reduce tar in syngas. Also, the highest gas yield and higher heating values (HHV) of syngas were achieved in the presence of dolomite for bench scale gasification of spent lignin pellets. In terms of producing tar-free syngas at a cheaper price, dolomite is a highly attractive catalyst. Similarly, Cortazar et al. [14] evaluated the effectiveness of dolomite, γ-alu-mina, olivine and FCC catalyst for continuous steam gasification of sawdust in a bench-scale plant equipped with a fountain confined conical spouted bed reactor It is noteworthy that in the presence of dolomite, hydrogen content is the highest in all the three cases presented which corresponds to lower tar content in the final syngas.

In this section, the impact of different catalyst on the kinetic energy from data stone will be assessed. The catalyst will match the same experiment as in Pinto et al. [13], as the dolomite, olivine and limestone will be tested. The dolomite was found to be the catalyst with the highest efficiency (Ea), as detailed in the following sections.

PRE-EXPERIMENT PREPARATIONS

Prior to the start of the experimentations, a few perquisites must be undertaken. This is in order to calibrate the device and ensure accurate readings from the TGA device, and the different effects on the date seeds.

In order to ensure the consistent operation of the of the TGA device and measure its uncertainty, 10 different date stone samples were prepared for testing in the TGA. Each of the samples was analysed at the same temperature rate and particle size at 20 ° C / min and 300 μm. The readings are shown on Figure (3)

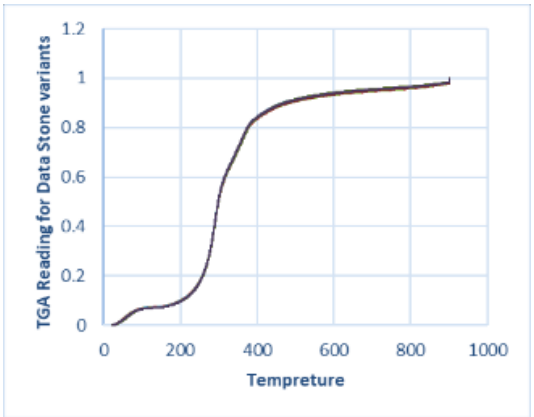

The readings were very similar for each sample of the date stone. This is illustrated in Figure (3) above, as the trend lines are visually identical throughout the testing for each date stone batch.

For further examination, sand was added to the data stones at different ratios. This is to determine the impact of non-catalytic materials on the procedure. The resultant readings are shown on Figure (4).

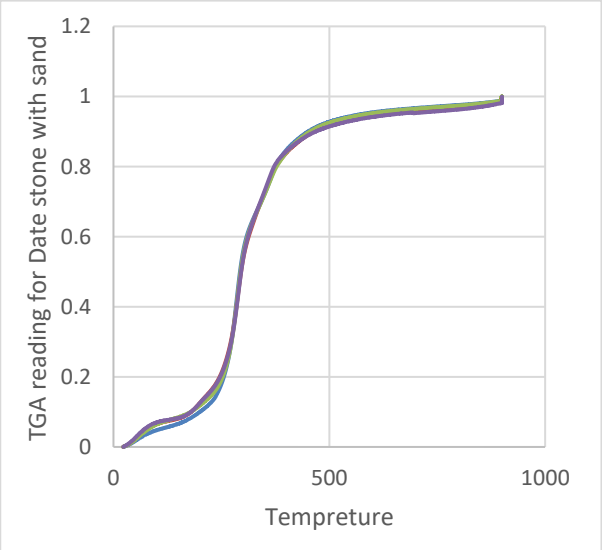

Figure 4 date stone with different ratio of sand

This has shown that sand had no impact whatsoever on the datestone, as it kept the same trend throughout the whole procedure as shown on the above graph. The rate date stone data is shown on the blue line, and then it is assessed against 10%, 20% and 30% (weight %) of sand mixed with the date stone. All the resultant trends are the identical to the original raw date stone.

Non-isothermal testing of date stone with different catalysts (dolomite, olivine and limestone) was done in the TGA instrument with a 20°C/min heating rate.

Several solid-state mechanisms, Table (1), were tested for a suitable fit by the Coats-Redfern method in order to determine the mechanisms responsible for the decomposition of biomass of particle size 710 μm at conversion between x=0.2-0.8, because the main conversion occurs in this study range. Equation (5-12) was applied separately to each model, the form of G(x) which gives a straight line with the highest correlation coefficient was considered to be the model function that best represents the kinetic mass loss reaction.

The TGA analysis for the of date stone with different kind of catalysts (dolomite, olivine, and limestone) was conducted using a Mettler Toledo TGA Series, model-TGA/DSC 3+ In this study, 9 mg of each date stone was weighed by a precision balance to the nearest 0.01mg and add 1 mg of catalyst.

Various catalysts were studied, but as mentioned above and in the literature, the dolomite is found to be the most effective[15]. The catalysts were assessed as 10% of (dolomite, olivine, and limestone) and through studying the kinetic energy fit via the Coats-Redfern method, with a focus on dolomite as the most efficient catalyst.

The resulting non-thermal TGA results as a function of G(x) is given in Table (3) below.

NON-ISOTHERMAL (TGA), X=0.2-0.8									
G(X)	G1	G2	G3	G4	G5	G6	G7	G8	G9
R2	0.82	0.85	0.14	0.64	0.14	0.91	0.88	0.88	0.88
G(X)	G11	G12	G13	G14	G15	G16	G17	G18	G19
R2	0.41	0.75	0.75	0.97	0.94	0.88	0.75	0.87	0.04

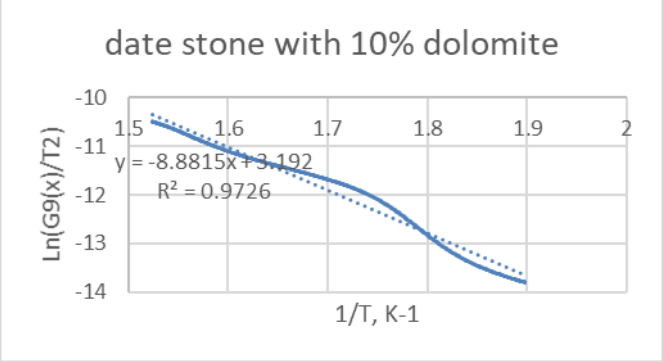

Figure 3 date stone with 10% dolomite

Similarly, the test was performed on both 10% olivine and 10% limestone, separately. The results for the first is shown on Figure (7), and for the latter in Figure (8). The data for each catalyst can then be utilised to estimate its efficiency (Ea), which subsequently would give a good indication about the effectiveness of the catalyst [11].

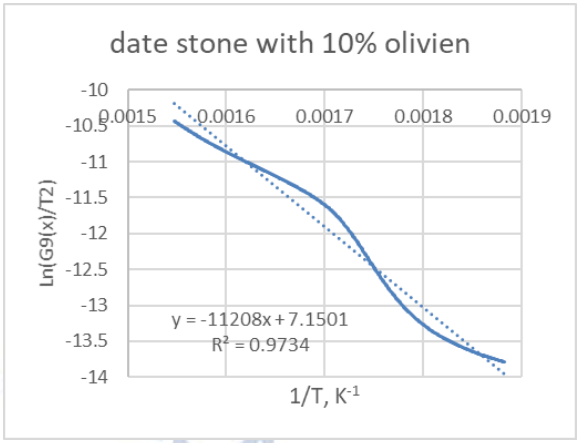

Figure 7 date stone with 10% olivine

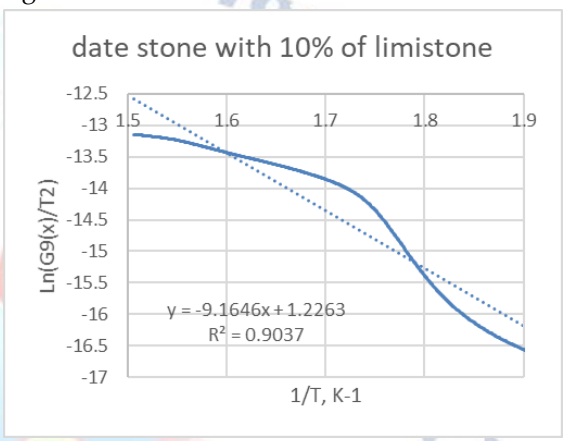

Figure 8 date stone with 10% of limestone

The calculated catalyst efficiency (Ea) for each of the dolomite, olivine and limestone is shown on Table (3) below, and it is clear that dolomite 10% (marked in blue) has the greatest effect on the process at 44.89 kJ/mole Ea.

Table4 Efficiency of potential catalyst for the gasification process

	Dolomite 10%	Olivine 10%	Limestone 10%
EA (kJ/MOLE)	44.8	95.12	76.19

Now that it is confirmed that dolomite is the more effective catalyst, by experiment as well as the literature, it is also important to ensure that the percentage weight of the added catalyst is optimum, and therefore this needs to be assessed as well. This will be discussed in the next section.

Effect of different ratio of dolomite as a catalyst.

Dolomite is a common rock-forming mineral with a specific gravity of 2.8 to 2.9, which is geographically extensive in underground geological deposits. Dolomite is calcium magnesium carbonate with a chemical formula of CaMg(CO3)2. The dolomites could be colourless, white, pink, green, grey, brown, or black [16].

In this part of the experiment the same conditions were used in the previous section, as follows: 20 ° C / min heating rate, nitrogen gas at a flow rate of 50 mL/min and the particle size for date stone is 710 μm.

Four samples were prepared and weighed to the nearest 0.01 mg of date kernel with different proportions of the first dolomite without adding dolomite, and the other samples by adding different percentages of 5%, 10% and 15% to find out the effective percentage of stimuli with the date stone.

Figure 9 Analysis of date stone.

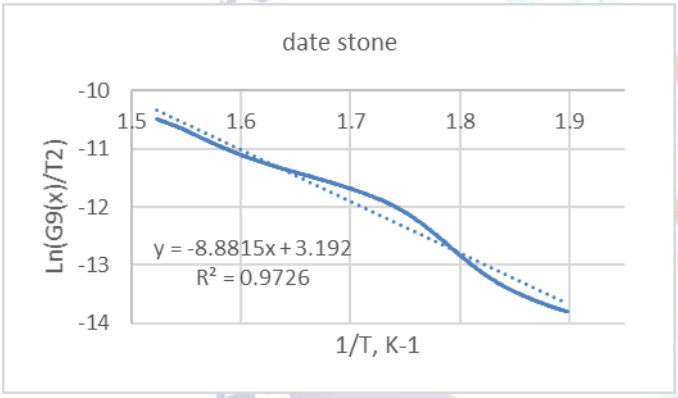

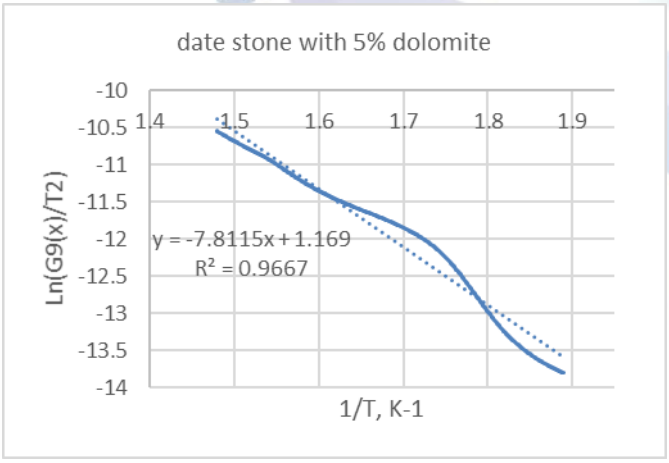

Figure 10 date stone with 5% dolomite.

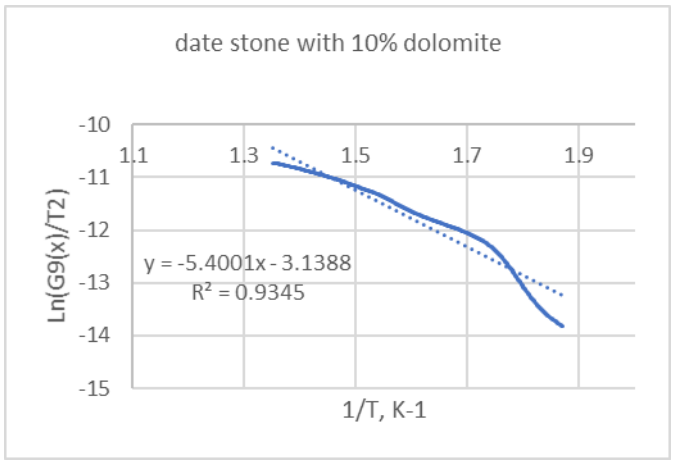

Figure 11 date stone with 10% dolomite.

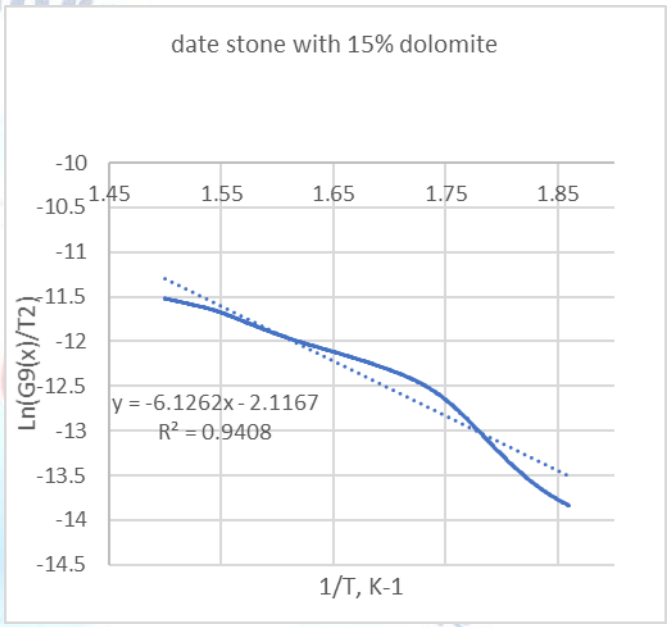

Figure 12 date stone with 15% dolomite.

Similarly, to the above approach – the dolomite was assessed at 15% weight and shown on Table (5) below as a function in G(x).

Table 1 The TGA reading for dolomite at 15% dolomite.

NON-ISOTHERMAL (TGA), X=0.2-0.8									
G(x)	G1	G2	G3	G4	G5	G6	G7	G8	G9
R2	0.84	0.86	0.37	0.66	0.37	0.91	0.89	0.89	0.89
G(X)	G11	G12	G13	G14	G15	G16	G17	G18	G19
R2	0.54	0.78	0.78	0.96	0.94	0.89	0.78	0.79	0.03

The same approach as above is taken to assess kinetic energy fit for dolomite at 10% and 15% via the Coats-Redfern method. The graphs obtained for the 10% dolomite is shown on Figure (11) and for the 15% dolomite in Figure (12). Although the trend line remains relatively the same, a 0.26% deviation between both ratios were detected.

The above data can then be taken to estimate the catalytic efficiency (Ea). This had been repeated for different dolomite percentage as a catalytic component in date stone reaction, namely for 5%, 10%, 15% and weightings. The full results are shown in Table (5-6) below, as the 10% dolomite is the most effective under the conditions tested. It had achieved the highest

Date 300µm	date	5%	10%	15%	20%
Ea	12.06	12.48	5.265	6.97	6.6

efficiency (Ea) at almost 44.89 kJ/mole, this is % higher than the 5% weighting for dolomite.

Table 6 The Ea value for different %wt dolomite catalyst.

In summary, the more efficient catalyst that will be used in this experiment is the 10% dolomite materiel with date stone, highlighted in blue in the table above.

Effect of particle sizes on the pyrolysis

The particle sizes can have a significant impact on the rate of reaction in a lab scale pyrolysis [16]. As the temperature gradients inside the particle is directly proportional to the particles size [16]. This indicates that the temperature of the surface is consistently higher than the core, and thus boosts the solid yields and reduces the gas and liquid yields [17].

Coats-Redfern method was used to estimate the apparent activation energies to enable quantification of the particle size and heating rate impact on the gasification of date stone.

As mentioned earlier, the sizes tested here are 300, 500 and 710 µm. The results are shown on Table (7) including efficiency obtained for each size. It can be seen that there is an impact of the particle size on efficiency exists, however it is relatively small.

Table 7 Ea corresponding to different particle sizes.

	Date 300µm	Date 500µm	Date 710µm
Ea	5.26	44.89	61.99

A directly proportional relationship between Ea and the particle size is observed on Table (5), as it had increased with the sample size increase.

Additionally, to the above, the impact of particle sizes on efficiency using the dolomite catalysts was investigated. The results are shown on Tables (8, 9 and 10). The results had shown the same trend as above, as the bigger the particle sizes the higher efficiency were obtained. The larger particle sizes result on narrower surface areas, and thus requires higher apparent activation energy to complete the process of pyrolysis. This is likely attributed to the irregular heating of the biomass samples as higher particle sizes result on late heating of inner portions of the sample [12].

Table 2 Date 300µm

Date 710µm				
	date	5%	10%	15%
Ea	73.84	64.94	44.89	50.93

Table 9 Date 500µm.isticated as PDF files are

Date 500µm	date	5%	10%	15%	20%
Ea (J/MOLE)	73.84	64.94	44.89	50.93	46.84

Date 710µm	date	5%	10%	15%	20%
Ea	82.80	73.58	61.99	65.91	55.39

Table 10 Date 710µm.

These results are aligned with the literature, as previous studies had shown that the efficiency increased with increasing the Lignocellulosic biomass particle sizes, according to Dadi et al. [12].

Another study had used hazelnut shells (from Turkish hazelnut) from the Black Sea in Turkey at similar non-isothermal conditions [18]. The study showed that the apparent activation energy value was reduced linearly with respect to the fraction of the particle size reduction. It was also observed that higher yield of char

was obtained at larger particle sizes, while higher apparent energy was also needed for the pyrolysis process.

Capsicum stalks were also tested by Y. Niu. Et al [19] via thermogravimetry differential gravimetric analysis. It was also shown that increasing the particle size, increased the reaction rate of pyrolysis.

CONCLUSION

The reaction kinetics of date stone biomass were measured using a TGA. The effectiveness of the TGA device was confirmed by testing ten samples of date stone and gave the same results. To make sure of the effect of the stimulating substances on the date stone, it was tested with different proportions of sand and the same results were given. And to choose the appropriate catalyst between (dolomite, olivine, and limestone) and the results indicated the effectiveness of dolomite with the date stone. The appropriate percentage of catalyst addition based on this study was 10% of the catalyst. In addition, the effect of the sample size was studied, and it was found that the smaller the size has the lower the value Ea.

REFERENCES

[1] Available: http://www.ijcea.org/papers/196-A028.pdf. [Accessed: 07-Oct-2020].

[2] W. H. Chen and P. C. Kuo, "A study on torrefaction of various biomass materials and its impact on lignocellulosic structure simulated by a thermogravimetry," Energy, vol. 35, no. 6, pp. 2580–2586, Jun. 2010.

[3] H. Yang, R. Yan, H. Chen, D. H. Lee, and C. Zheng, "Characteristics of hemicellulose, cellulose and lignin pyrolysis," Fuel, vol. 86, no. 12–13, pp. 1781–1788, Aug. 2007.

[4] E. Kastanaki, D. Vamvuka, P. Grammelis, and E. Kakaras, "Thermogravimetric studies of the behavior of lignite-biomass blends during devolatilization," Fuel Process. Technol., vol. 77–78, pp. 159–166, Jun. 2002.

[5] J. Jae et al., "Depolymerization of lignocellulosic biomass to fuel precursors: Maximizing carbon efficiency by combining hydrolysis with pyrolysis," in Energy and Environmental Science, 2010, vol. 3, no. 3, pp. 358–365.

[6] C. Gai, Y. Dong, Z. Lv, Z. Zhang, J. Liang, and Y. Liu, "Pyrolysis behavior and kinetic study of phenol as tar model compound in micro fluidized bed reactor," Int. J. Hydrogen Energy, vol. 40, no. 25, pp. 7956–7964, Jul. 2015.

[7] M. R. B. Guerrero et al., "Thermogravimetric study on the pyrolysis kinetics of apple pomace as waste biomass," Int. J. Hydrogen Energy, vol. 39, no. 29, pp. 16619–16627, 2014.

[8] "Principles of Thermal Analysis and Calorimetry - كتب Google." [Online]. Available: https://books.google.co.uk/books?hl=ar&lr=&id=obarDwAAQBAJ&oi=fnd&pg=PA72&dq=P.+J.+Haines,+%22Principles+of+thermal+analysis+and+calorimetry-Royal+society+of+chemistry,%22+pp.+42-47,+2002.&ots=zfuTgBCSfz&sig=bjs2Q3M0HmeXgCC16CKvnkO7wAk&redir_esc=y#v=onepage&q&f=false. [Accessed: 07-Nov-2020].

[9] J. Yu et al., "Isothermal differential characteristics of gas-solid reaction in micro-fluidized bed reactor," in Fuel, 2013, vol. 103, pp. 29–36.

[10] K. Oluoti, T. Richards, T. R. K. Doddapaneni, and D. Kanagasabapathi, "Evaluation of the pyrolysis and gasification kinetics of tropical wood biomass," BioResources, vol. 9, no. 2, pp. 2179–2190, 2014.

[11] J. M. Encinar, J. F. González, and J. González, "Fixed-bed pyrolysis of Cynara cardunculus L. Product yields and compositions," Fuel Process. Technol., vol. 68, no. 3, pp. 209–222, 2000.

[12] G. Gözke and K. Açıkalın, "Pyrolysis characteristics and kinetics of sour cherry stalk and flesh via thermogravimetric analysis using isoconversional methods," J. Therm. Anal. Calorim., 2020.

[13] F. Pinto et al., "Effects of experimental conditions and of addition of natural minerals on syngas production from lignin by oxy-gasification: Comparison of bench- and pilot scale gasification," Fuel, vol. 140, pp. 62–72, Jan. 2015.

[14] M. Cortazar, G. Lopez, J. Alvarez, M. Amutio, J. Bilbao, and M. Olazar, "Behaviour of primary catalysts in the biomass steam gasification in a fountain confined spouted bed," Fuel, vol. 253, pp. 1446–1456, Oct. 2019.

[15] "Dolomite Mineral | Uses and Properties." [Online]. Available: https://geology.com/minerals/dolomite.shtml. [Accessed: 26-Nov-2020].

[16] J. M. Encinar, J. F. González, and J. González, "Fixed-bed pyrolysis of Cynara cardunculus L. Product yields and compositions," Fuel Process. Technol., vol. 68, no. 3, pp. 209–222, Dec. 2000.

[17] G. Gözke and K. Açıkalın, "Pyrolysis characteristics and kinetics of sour cherry stalk and flesh via thermogravimetric analysis using isoconversional methods," J. Therm. Anal. Calorim., no. 0123456789, 2020.

[18] H. Haykiri-Acma, "The role of particle size in the non-isothermal pyrolysis of hazelnut shell," J. Anal. Appl. Pyrolysis, vol. 75, no. 2, pp. 211–216, Mar. 2006.

[19] Y. Niu, H. Tan, Y. Liu, X. Wang, and T. Xu, "The effect of particle size and heating rate on pyrolysis of waste

capsicum stalks biomass," Energy Sources, Part A Recover. Util. Environ. Eff., vol. 35, no. 17, pp. 1663–1669, Sep. 2013.